AN OPPOSED DIFFERENCING SCHEME FOR SOLVING THE INCOMPRESSIBLE NAVIER-STOKES EQUATIONS

Marcelo Reggio and Ricardo Camarero

EPM/RT-86-43

(1986)

EPM/RT-86-43

AN OPPOSED DIFFERENCING SCHEME FOR SOLVING THE INCOMPRESSIBLE NAVIER-STOKES EQUATIONS

Marcelo Reggio and Ricardo Camarero

Ecole Polytechnique de Montréal

OCTOBER 1986

This work was carried out with the financial support of the the NSERC of Canada and the Ministère de la Science et Technologie du Quebec.

Dépot légal , 4e trimestre 1986
Blibliothèque nationale du Québec
Blibliothèque nationale du Canada

Pour se procurer une copie de ce document, s'adresser au:

Service de l'édition
Ecole Polytechnique de Montréal
Case Postale 6079, Succ. "A"
Montréal,Québec H3C 3A7
(514) 340-4903

Compter 0,05$ par page(arrondir au dollar le plus près),plus 1,50$(Canada) ou 2,50$(étranger) pour la couverture,les frais de poste et la manutention.Régler en dollars canadiens par chèque ou mandat-poste au nom de l'Ecole Polytechnique de Montréal.Nous n'honorerons que les commandes accompagnées d'un paiement,sauf s'il y a eu entente préalable, dans le cas d'établissements d'enseignement ou d'organismes canadiens.

SUMMARY

A numerical scheme is developed for the solution of the unsteady, two dimensional, incompressible Navier-Stokes equations in generalized coordinates. The governing equations written in the conservation form, are formulated in terms of pressure and velocity. The scheme is based on a combination of forward and backward differencing for the spatial derivatives of the flux and the pressure. This characteristic allows the use of a single computational cell for the continuity and momentum balances, together with the storage of the pressure and the velocity components at the center of this calculation element. The resulting algorithm shows no oscillations on the velocity or pressure fields. Computing is made for a series of channel flows containing constrictions and enlargements.

1. INTRODUCTION

Finite-volume procedures for the solution of the primitive-variable form of the incompressible Navier-Stokes equations in a general geometry, are based on the subdivision of the solution domain into discrete volumes and applying the conservation laws over these elements. In this methodology three main aspects can be distinguished: the domain discretization technique, the choice of a computational element for the storage location for the dependent variables, and the coupling between the continuity and momentum equations.

A critical factor in the development of an accurate numerical procedure for the solution of fluid flow problems in general shapes, is the choice of an appropriate coordinate system. Among the different techniques that can be used to numerically discretize the domain of interest, the body-conforming method[1,2] has been retained. In this approach the governing transport equations are formulated for a curvilinear coordinate system, where the geometric characteristics of the problem are intrinsically imbedded in generalized equations.

The second aspect, the construction of an efficient computational cell has been attempted by different means, among them the staggered grid method[3] is the most widely used. As an alternative, in Ref[4] a scheme using an opposed differencing technique in the main flow direction combined with an overlapping mesh in the secondary direction has been presented. This procedure prevents spurious oscillations in the pressure field. In spite of this

particular discretization, it can be shown that such a method can only be regarded as partially nonstaggered. This is because of the requirement of an overlapping configuration in the secondary direction.

In the present study, it is proposed to employ a completely nonstaggered discretization by applying the opposed differencing idea to both directions. This yields a grid twice as fine in the secondary direction, as well as allowing the removal of the restriction of an odd number of grid points in that direction. As a result the location of the physical properties are calculated at the center of the same computational cell used for both the momemtum and the continuity balances.

Finally, the most difficult aspect associated with the solution of the incompressible Navier-Stokes equations in primitive variables, is perhaps the constraint $\nabla V=0$ that has to be satisfied everywhere. In the present effort this p-v coupling problem has been treated by two alternative approaches. Both have in common a pressure equation derived from the continuity and linearised momentum equations in a manner similar to that proposed by the SIMPLE method[5]. Their difference lies in the way that the pressure adjustement is regarded and applied.

The first method is based on a semi-implicit procedure, where only the pressure gradient terms are treated implicitly on the momentum equations; and with the continuity relation enforced at every time step within a prescribed tolerance. In this case the

unsteady process is correctly followed.

In the second case, the pressure correction equation is regarded as an artificial continuity equation[6], that relates the pressure and velocity fields. In that instance the process does not follow the transient evolution; however the solution is meaningful when the steady state is reached

2.EQUATIONS OF MOTION.

When solving the equations of motion on a curvilinear coordinate system, one may retain as dependent variables, either velocity components along the curvilinear directions, or cartesian velocity components. If the latter is chosen, the resulting system which is not significantly more complex than their cartesian counterpart, remains in the conservation law form, and the discrete approximations can be easily handled.

With this approach, the time dependent Navier-Stokes equations can be written in conservative form as:

$$\frac{\partial q}{\partial t} + \frac{\partial E}{\partial \xi} + \frac{\partial F}{\partial \eta} = \frac{\partial R}{\partial \xi} + \frac{\partial S}{\partial \eta} \qquad (1)$$

where:

$$q = J\begin{bmatrix} 0 \\ u \\ v \end{bmatrix} \qquad E = J\begin{bmatrix} U \\ uU + p\xi_x \\ vU + p\xi_y \end{bmatrix} \qquad F = J\begin{bmatrix} V \\ uV + p\eta_x \\ vV + p\eta_y \end{bmatrix}$$

$$R = J/R_e\begin{bmatrix} 0 \\ g^{11}u_\xi + g^{12}u_\eta \\ g^{11}v_\xi + g^{12}v_\eta \end{bmatrix} \qquad S = J/R_e\begin{bmatrix} 0 \\ g^{21}u_\xi + g^{22}u_\eta \\ g^{21}v_\xi + g^{22}v_\eta \end{bmatrix}$$

and $R_e=(\rho u_o L/\mu)$, with u_o and L beeing reference values.

The curvilinear velocity components U,V and the cartesian velocity components u,v are related by:

$$U = u\xi_x + v\xi_y$$

$$V = u\eta_x + v\eta_y \qquad (2)$$

The metric terms $\xi_x, \xi_y, \eta_x, \eta_y$, the jacobian J and the contravariant metric tensor components g^{11}, g^{12}, g^{21}, and g^{22} are obtained from:

$$\xi_x = y_\eta/J, \qquad \xi_y = -x_\eta/J$$

$$\eta_x = -y_\xi/J, \qquad \eta_y = x_\xi/J$$

$$J = x_\xi y_\eta - x_\eta y_\xi$$

$$g^{11} = \xi_x^2 + \xi_y^2 \qquad g^{12} = \xi_x \eta_x + \xi_y \eta_y$$

$$g^{21} = g^{12} \qquad g^{22} = \eta_x^2 + \eta_y^2$$

3. DISCRETE FORMULATION

The temporal scheme used here is explicit, although it is only first order accurate, it has been chosen because of the simplicity of its implementation. In compact form can be written as:

$$\Delta q + \Delta t (E_\xi + F_\eta)^n = \Delta t (R_\xi + S_\eta)^n$$

where Δ denotes the forward time difference operator and n the time level.

Attention is now focused on the construction of the computational cell, that is the storage and the approximation of the spatial derivatives of the physical properties. The values of the pressure and cartesian velocity components u and v, are defined at the cell center (i+1/2,j+1/2) which is used for both mass and momentum

calculations, as shown in Fig.1. On the other hand, the curvilinear velocity components U and V are located at the center of the faces (i,j+1/2), (i+1,j+1/2) and (i+1/2,j),(i+1/2,j+1) respectively.

It is well known, that the unknown properties at the cell faces cannot be linearly interpolated, as checkerboard fields would arise. In the present approach, this problem is solved by applying a combination of forward and backward differencing for mass and pressure respectively, along with the use of the weighted upstream difference scheme of Raithby and Torrance[7] for the convected momentum fluxes and diffusion terms.

In the ξ direction, mass gradients are obtained by upwind differencing, so the flux through the downwind face i+1 is controlled by the velocity at the center i+1/2,j+1/2 of the element. Pressure gradients on the other hand, are calculated via downwind differences, that is to say, the pressure located at the cell center i+1/2,j+1/2 has to be regarded as acting on the upstream face i.

In the η direction, and in order to avoid numerical errors due to asymmetry, a sligthly different treatment is applied. This implies a global procedure composed of a series of predictor-corrector steps where the the forward-backward combination is applied in reverse ways for successive time levels.

In a first step of the computation, upwinding differencing is used for mass combined with downwinding for pressure. This is followed by a corrector step, where downwind differencing for mass together

with upwinding for pressure is employed.

These ideas, are now to be applied to the discrete analog of the transport equations.

The discrete form of the continuity constraint, represented by Eq.(1) can be written as:

$$\frac{(JU)_{i+1,j+1/2} - (JU)_{i,j+1/2}}{\Delta\xi} + \frac{(JV)_{i+1/2,j+1} - (JV)_{i+1/2,j}}{\Delta\eta} = 0 \qquad (3)$$

This equation only involves the curvilinear U and V velocity components at the locations i,j+1/2;i+1,j+1/2 and i+1/2,j;i+1/2,j+1 respectively. These are obtained via the discrete form of Eq.(2), where the cartesian velocity components appear. These physical properties, that are calculated from the momentum equations, are not available at the above mentioned stations, but rather at the center of the computational cell (i+1/2,j+1/2). However, as a result of the opposed differencing procedure in both directions the curvilinear components are obtained from Eq.(2) as:

i) for the U components

$$U_{i,j+1/2} = u_{i-1/2,j+1/2}(\eta_x)_{i,j} + v_{i-1/2,j+1/2}(\eta_y)_{i,j} \qquad (4a)$$

$$U_{i+1,j+1/2} = u_{i+1/2,j+1/2}(\eta_x)_{i+1,j} + v_{i+1/2,j+1/2}(\eta_y)_{i+1,j}$$

ii) for the V components

$$V_{i+1/2,j} = u_{i+1/2,j-1/2}(\eta_x)_{i,j} + v_{i+1/2,j-1/2}(\eta_y)_{i,j}$$

$$V_{i+1/2,j+1} = u_{i+1/2,j+1/2}(\eta_x)_{i,j+1} + v_{i+1/2,j+1/2}(\eta_y)_{i,j+1} \quad (4b)$$

for an even step; and

$$V_{i+1/2,j} = u_{i+1/2,j+1/2}(\eta_x)_{i,j} + v_{i+1/2,j+1/2}(\eta_y)_{i,j}$$

$$V_{i+1/2,j+1} = u_{i+1/2,j+3/2}(\eta_x)_{i,j+1} + v_{i+1/2,j+3/2}(\eta_y)_{i,j+1} \quad (4c)$$

for an odd step.

where upwinding(or downwinding) is used independently of the signs of u or v.

The discrete form of the momentum equations also requires the knowledge of the convected momentum fluxes and diffusion terms at the cell faces; these terms are evaluated in a similar way as in Ref[4] by employing the weighted upstream difference scheme[7]

As mentioned earlier, the forward-backward differencing for mass flow and pressure in the ξ direction , is reversed in the η direction for succesive time levels. With this particularity, alternate momentum equations are used for odd and even steps. An example of the discrete form of this equations is given in Appendix A.

4.SOLUTION PROCEDURE

The general algorithm is based on the iterative solution of a set of equations for the individual variables. The sequence of calculations can be outlined as follows.

First, pressure, cartesian and corresponding curvilinear velocity fields are guessed. Then, cartesian velocity increments are obtained by solving the linearised form of the momentum equations. These resulting changes, located at the cell center, and denoted by δu^* and δv^*, are then substitued into equations (4a) and (4b) or (4c) to compute the corresponding contravariant velocity increments δU^* and δV^* at the cell faces. These intermediate values that do not satisfy mass conservation, are finally added to the existing curvilinear components U and V, resulting in modified values denoted by U^* and V^*, which also do not verify the zero-divergence condition.

To correct these U^* and V^* components so as to yield a pressure field which drives velocities that satisfy both the momentum and the

continuity equations simultaneously, a pressure equation is derived from the discretized form of these equations. The derivation of this equation follows standard procedures[5,8] which have been modified for a curvilinear mesh and employed in earlier work[4].

By writing the discrete form of the momentum equations twice, once for the intermediate fields u^*, v^* and p^*, and then for the corrected fields $u = u^* + \delta u$; $v = v^* + \delta v$; $p = p^* + \delta p$, with u and v meeting mass conservation; cartesian $\delta u, \delta v$ and subsequent contravariant velocity corrections $\delta U, \delta V$ can be approximated in terms of pressure corrections as follows:

$$\delta U = f^{u} \delta p$$

$$\delta V = f^{v} \delta p$$

These values that depend on the pressure changes δp, also have to respect the conservation of mass, consequently they are substituted into an equivalent form of Eq.3, leading to a pressure correction equation that can be abbreviated as:

$$\delta p = -\lambda D / \Delta t \qquad (5)$$

where D denotes a mass souce term (or continuity imbalance), and λ a convergence parameter that is function of the geometry of each cell.

Once the pressure adjustement $\delta p = p - p^*$, and the consequent curvilinear velocity corrections $\delta V = U - U^*$, $\delta V = V - V^*$ are calculated, the provisional velocity and pressure fields U^*, V^* and p^* are simply

rectified by:

$$U = U^* + \delta U$$

$$V = V^* + \delta V$$

$$p = p^* + \delta p$$

At this stage two distinct procedures were followed to modify these variables.

a) Approximate pressure correction equation

In this instance, a MAC-type technique[9] was employed to iteratively update the pressure over the entire computational domain as:

$$p_{m+1} = p_m - \lambda \nabla V_m/\Delta t \qquad (6)$$

This is carried out by applying a cell by cell sweep in the inlet-outlet direction, until the difference of the pressure between two successive iterations steps m and m+1 is less than a prescribed limit; and consequently the continuity constraint is satisfied.

b) Artificial Compressibility

This method described by Chorin[6] circumvents the traditional problem in incompressible calculations, by adding a time derivative of an artificial density to the continuity equation. This artifice turns the incompressible equations into an hyperbolic system. With such an

artificial compressibility term added, together with the use of a state law defined by $p = c^2\rho$, where c^2 represents a convergence parameter, the perturbed continuity equation can now be expressed as:

$$\frac{\partial p}{\partial t} + c^2 \nabla \cdot V = 0 \qquad (7)$$

Adopting a forward time difference approximation as used previously, the discrete form of the pressure equation gives:

$$p^{n+1} = p^n - \Delta t c^2 \nabla \cdot V^{n+1} \qquad (8)$$

Whith this technique, the resulting scheme is obviously no longer consistent during the transient stage, and the solution will only represent the flow in the asymptotic limit of the steady state.

As pointed out by Ref[10], it is interesting to note that a relation can be established between the pressure modification given by Eq.(8) and the pressure correction represented by Eq.(6), which is solved by a simple Jacoby-type procedure. Comparing these two equations, one can conclude that if at each time step the pressure correction Eq.(6) is not enforced to satisfy $\nabla \cdot V \to 0$, but only one iteration is made, then the pressure correction method becomes the density correction procedure with $\lambda = c^2 \Delta t^2$.

It can be appreciated from this last relation, that the quantiy c^2 depends on λ which is in turn is a function of the geometry of each cell. As a consequence, the term c^2 employed in the present development, is not a constant as is generally the case when applying

the artificial compressibility idea; and all the contributing parameters on the state law $p = \rho c^2$ vary from point-to-point

After one or several iterations are done, depending on the selected approach, the cartesian velocity components are decoded and the boundary conditions applied. Finally the time level is advanced and the cycle repeated until the steady state is reached.

Both, the artificial density and pressure correction approaches, were applied to exploratory test cases; however no significant differences were noted in the required CPU time to obtain a converged flow field.

5. APPLICATIONS

5.1 Flow between parallel plates.

The first case chosen for the validation of the method was that of the developing laminar flow between two parallel plates. For this type of flow a parabolic profile is expected to be formed at about 0.04Re[11], with the Reynolds number based on the width of the channel; so computations were made in a channel with a length to width ratio L/D=10 for Re=100, using a 63x15 grid.

Fig.2a shows the predicted centerline velocity behaviour as function of the distance from the inlet. The maximum attained value agrees well with the analytical value of 1.5. Fig.2b depicts the pressure at the wall as function of the normalized length. The

calculated slope of $\Delta p/\Delta x=-.128$ of the pressure gradient compares very well with the value of $-12/Re$ from the analytical solution. On Fig.2c, the calculated velocity profile just before the outlet (full line) is compared with the analytical solution $u(y)=6(y-y^2)$ (dashed lines). The results indicate a good agreement between both solutions.

5.2 Asymmetric Constriction

The second problem analyzed is the flow in a channel with an asymmetric constriction. The geometric characteristics of the selected model were devised by Ref[12] which uses a conformal coordinate transformation to generate a family of channel configurations. The chosen duct has been fully tested by that author, using the vorticity-stream function form of the Navier-Stokes equations.

At the inlet a developed profile is assumed, the discretization uses a 63x23 grid and tests up to Re=1000 were conducted. Figs.3a and 3b provide a velocity vector plot and stream-function contours for Re=1000. Examination of these illustrations clearly reveals a reversed flow region which increases with Reynolds number. The qualitative agreement of these last figures with those reported by Ref.[12] is good; however a detailed comparison disclose some discrepancies. In particular those concerning the separation and reattachement points.

In the present calculations no separation appears for Re=100, as found by Ref[12]. For a Reynolds number of 1000 the respective separation and reattachement points predicted by the current computation, at the 0.43 and 2.45 x locations (referred to the maximun

of the constriction) do not coincide with the estimated values of 0.19 and 3.75 of Ref[12]. With no experimental data available for this geometry it is no possible to infer the better result.

5.3 Sinusoidal passage

In order to verify the scheme's stability in a more complex geometry, the flow in a double-sinus channel was studied. The discretization uses a 63x15 grid, with a developed velocity profile imposed at the inlet, and a Reynolds number of 100.

Fig.4a illustrates the calculated velocity field, while Figs.4b and 4c present the corresponding steamlines and isobar contours respectively. One can notice the formation of five distinct recirculation bubbles; the last of them is the result of the oscillatory movement of the fluid downstream of the distorted zone. This movement finally dies out due to the viscous effects.

The complexity of the pressure behaviour can be appreciated on Fig.4d, in which the pressure at the bottom (full line) and top walls (dashed lines) is plotted as a function of the distance from the inlet. This result shows a shitfed periodic pattern of such parameter between the upper and lower walls, as qualitatively expected.

5.4 Jeffery-Hamel Flow

The problem of the flow between nonparallel plane walls due to a

line source, known as the Jeffery-Hamel flow was next investigated. The divergent duct considered for the numerical calculation was chosen after a test case studied by Ref[13] and as is illustrated in Fig.5a, where a total angle of 10° is used for the divergence of the walls. At the inlet one imposes a velocity profile corresponding to the analytical solution[14,15] for Re=684 defined as $Re=u_{max}r/\upsilon$, u_{max} being the velocity along the axial streamline and r the radial position. The discretization was carried out with 63x19 grid points

For this geometry, tests were conducted for two different Reynolds numbers.

Fig.5b illustrates the calculated (full line) and analytical (square symbols) velocity profile u/u_{max} for Re=684. This remains constant along the duct axis and the section selected for the representation is that of the oulet. As expected both profiles agree well since the flow does not separate.

A second test was conducted for Re=2500, with the same inlet profile used for the preceeding case. On Fig.5c is shown the computed (full line) and analytical (squares) normalized velocity profiles [15]. Compared to the previous example, both velocity profiles sharpen up in the center with accompanying backflow regions near the walls that match reasonably well with each other.

NOMENCLATURE

c	convergence parameter on the artificial equation of state
C_p	pressure coefficient
D	continuity imbalance
E,F	flux vectors in ξ and η coordinate directions
g^{ij}	metric tensor components
J	Jacobian of transformation matrix
L	characteristic length
p	pressure
p^*	estimated pressure
q	vector of conservation variables
R,S	viscous flux terms in ξ and η coordinate directions
R_e	Reynolds number
t	time
u,v	velocity components in x and y directions
u^*,v^*	estimated cartesian velocity field
U,V	contravariant velocity components in ξ and η directions
U^*,V^*	tentative curvilinear velocity components
x,y	Cartesian coordinates
ξ,η	curvilinear coordinates
δp	pressure correction
Δt	time step
$\delta u,\delta v$	Cartesian velocity corrections
$\delta U,\delta V$	contravariant velocity corrections
λ	geometric parameter

Subscripts

m	iteration step
x, y ξ, η	first partial differentiation
i,j	variable location
0	reference value

Superscript

n	time level

APPENDIX A

Let us denote the discretized time dependent, flux, and viscous terms of the u momentum equation as:

$$A_p = J_{i+1/2,j+1/2} \frac{(u^{n+1}-u^n)_{i+1/2,j+1/2}}{\Delta t}$$

$$A_{nb} = \frac{(JuU)_{i+1,j+1/2} - (JuU)_{i,j+1/2}}{\Delta \xi} + \frac{(JuV)_{i+1/2,j+1} - (JuV)_{i+1/2,j}}{\Delta \eta}$$

$$S_{nb} = \frac{C_{i,j+1/2} - C_{i+1,j+1/2}}{\Delta \xi} + \frac{C_{i+1/2,j} - C_{i+1/2,j+1}}{\Delta \eta}$$

Then the conservation equations are written:

i) for an even time level

$$A_p + A_{nb} + S_{nb} + P_{nbe} = 0 \qquad (A1)$$

where P_{nbe} is calculated by,

$$P_{nbe} = \frac{\rho_{i+3/2,j+1/2}(J\xi_x)_{i+1,j+1/2} - \rho_{i+1/2,j+1/2}(J\xi_x)_{i,j+1/2}}{\Delta\xi}$$

$$+ \frac{\rho_{i+1/2,j+3/2}(J\eta_x)_{i+1/2,j+1} - \rho_{i+1/2,j+1/2}(J\eta_x)_{i+1/2,j}}{\Delta\eta}$$

and with U and V appearing in the A_{nb} expression calculated by Eqs 4a and 4b respectively; and

ii) for an odd time level

$$A_p + A_{nb} + S_{nb} + P_{nbo} = 0 \qquad (A2)$$

with P_{nbo} computed by:

$$P_{nbo} = \frac{\rho_{i+3/2,j+1/2}(J\xi_x)_{i+1,j+1/2} - \rho_{i+1/2,j+1/2}(J\xi_x)_{i,j+1/2}}{\Delta\xi}$$

$$+ \frac{\rho_{i+1/2,j+1/2}(J\eta_x)_{i+1/2,j+1} - \rho_{i+1/2,j-1/2}(J\eta_x)_{i+1/2,j}}{\Delta\eta}$$

where U and V are obtained through Eqs 4a and 4c respectively.

REFERENCES:

1. Thompson J.F., Thames F.C., and Mastin C.W., "Automatic Numerical Generation of Body-Fitted Curvilinear Coordinate System for Fields Containing Any Number of Arbitrary Two-Dimensional Bodies", Journal of Computational Physics, vol 15, p.229, 1984

2. Camarero R., Ozell B., Reggio M., and Garon A., "Introduction to Grid Generation in Turbomachinery," VKI Lecture Serie 2, Numerical Techniques for Viscous Calculations in Turbomachinery Jan.20-24,1986

3. Harlow F.H and Welch J.E., "Numerical Calculation of Time-Dependent Viscous Incompressible Flow of Fluid with Free Surface", Phys.Fluids, Vol. 8, no 12, pp. 2182-2189, 1965

4. Reggio M. and Camarero R., "Numerical Solution Procedure for Viscous Incompressible Flows" Numerical Heat Transfer Vol. 10, 1986.

5. Patankar S.V., "Numerical Heat Transfer and Fluid Flow" Hemisphere Publishing Corporation, Washington.,1980

6. Chorin A.J., " A Numerical Method for Solving Incompressible Viscous Flow Problems" J.Comp.Phys. 2, pp.12-26, 1967.

7. Raithby G.D. and Torrance K.E., "Upstream-Weighted Differencing Schemes and their Application to Elliptic Problems Involving Fluid Flow", Computer Fluids vol. 2, pp 191-206, 1974

8. Connell S.D. and Stow P. "The Pressure Correction Method", Computers & Fluids Vol. 14, No. 1, pp.1-10, 1986.

9. Hirt C.W., Nichols B.D. and Romero N.C., " SOLA- A Numerical Solution Algorithm for Transient Fluid Flows", 1975, Los Alamos Scientific Labortory,Report LA-5852,1975

10. Peyret R. and Taylor T.D, "Computational Methods for Fluid Flow" Springer Verlag New York, 1985

11.Schlichting H.,"Boundary-Layer Theory", seventh ed.,McGraw Hill, 1979.

12. Oswald G.A., "A Direct Numerical Method for the Solution of Unsteady Navier-Stokes Equations in Generalized Orthogonal Coordinates", Ph.D. Thesis, University of Cincinnati, 1983

13. Maliska C.R.,"A Solution Method for Three-Dimensional Parabolic Fluid Flow Problems in Nonorthogonal Coordinates", Ph.D. Thesis, University of Waterloo,Canada,1981

14. Millsaps K. and Pohlhausen K., "Thermal Distribution in Jeffery-Hamel Flows Between Nonparallel Plane Walls" Journal of the Aeronautical Sciences, pp.187-196, 1953.

15. Lu P-C., "Introduction to the Mechanics of Viscous Fluids", Hemisphere Publishing Corporation, 1977.

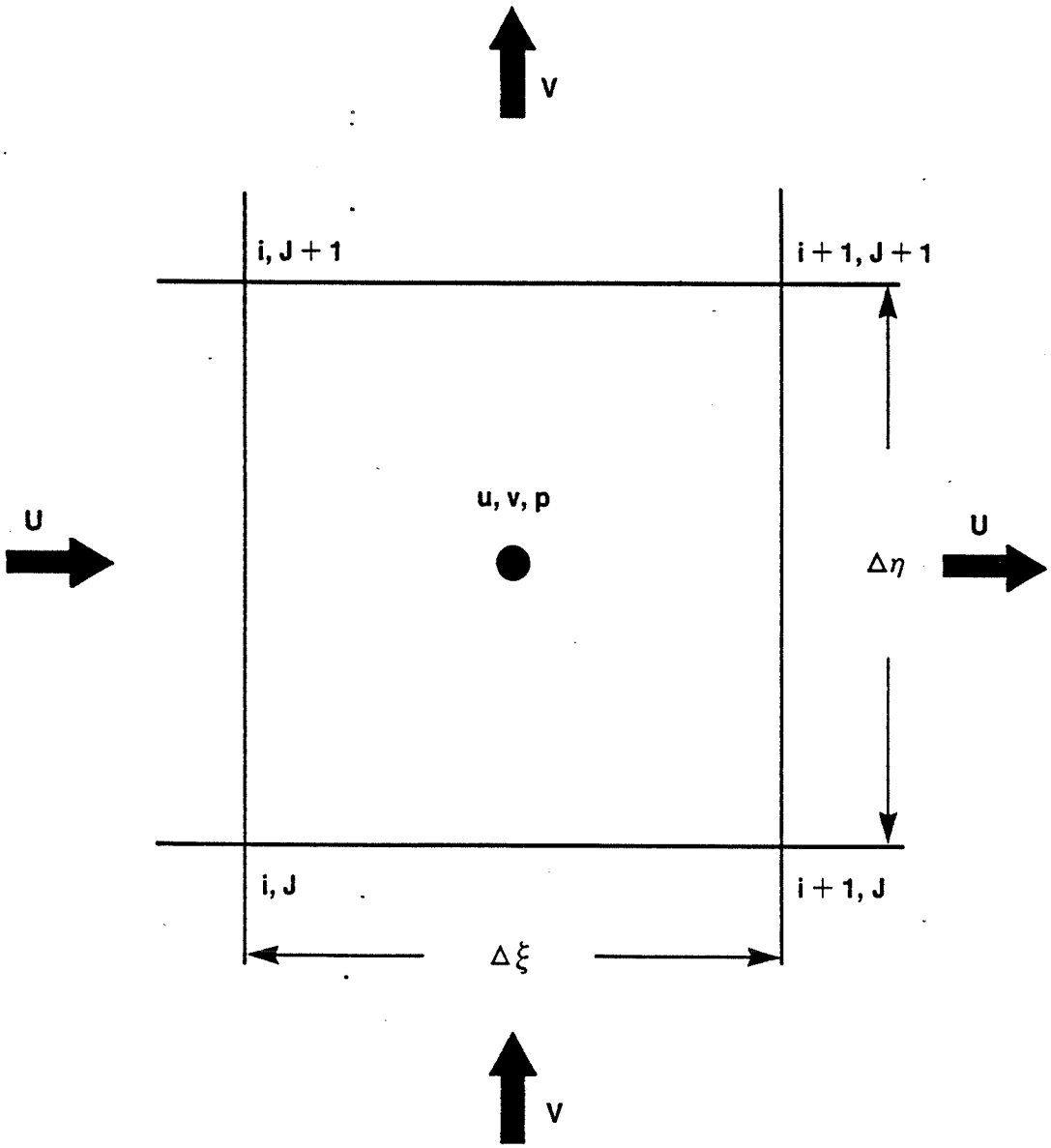

Fig. 1 Basic computational cell

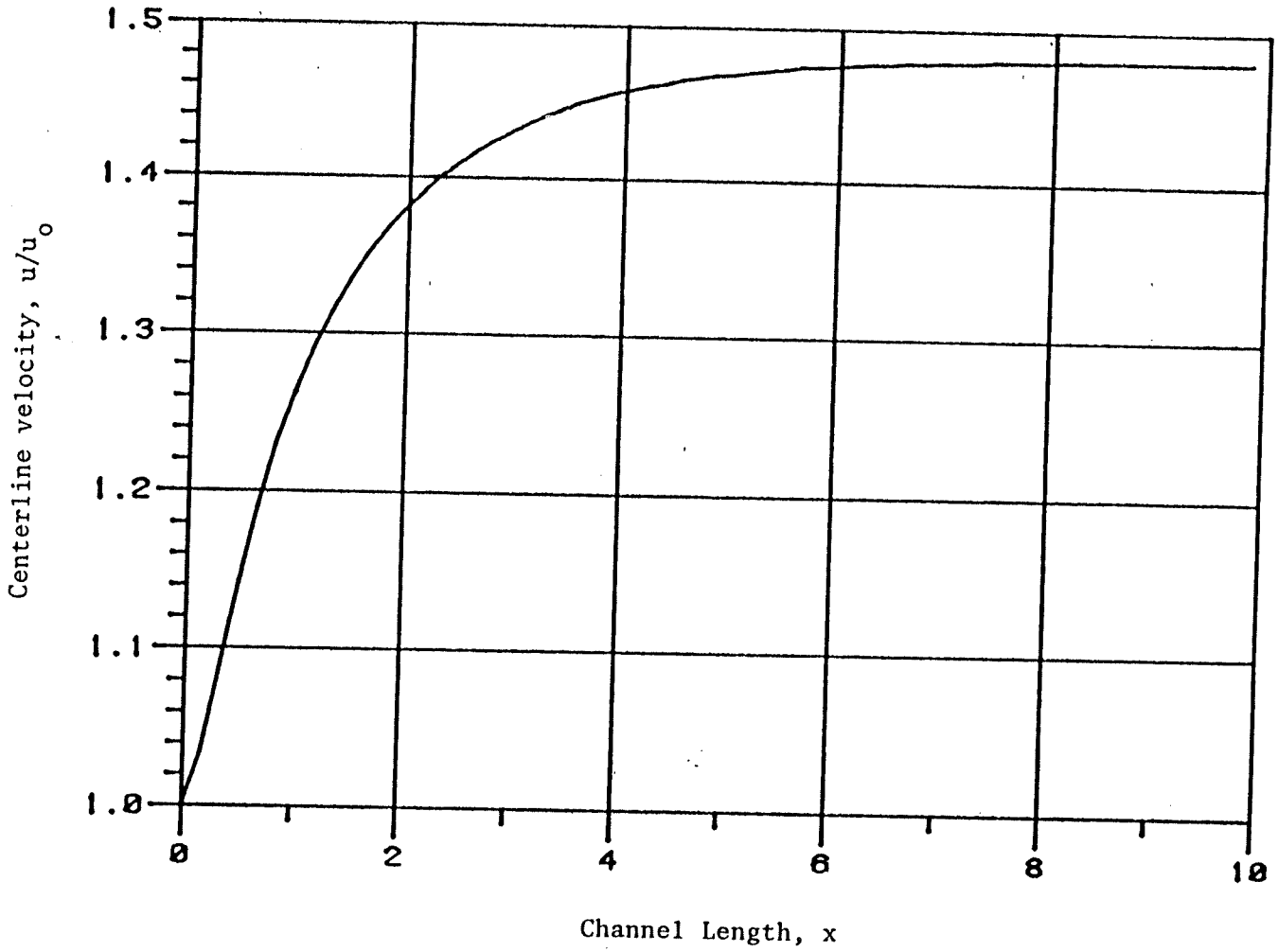

Fig. 2a Centerline velocity evolution for Re=100

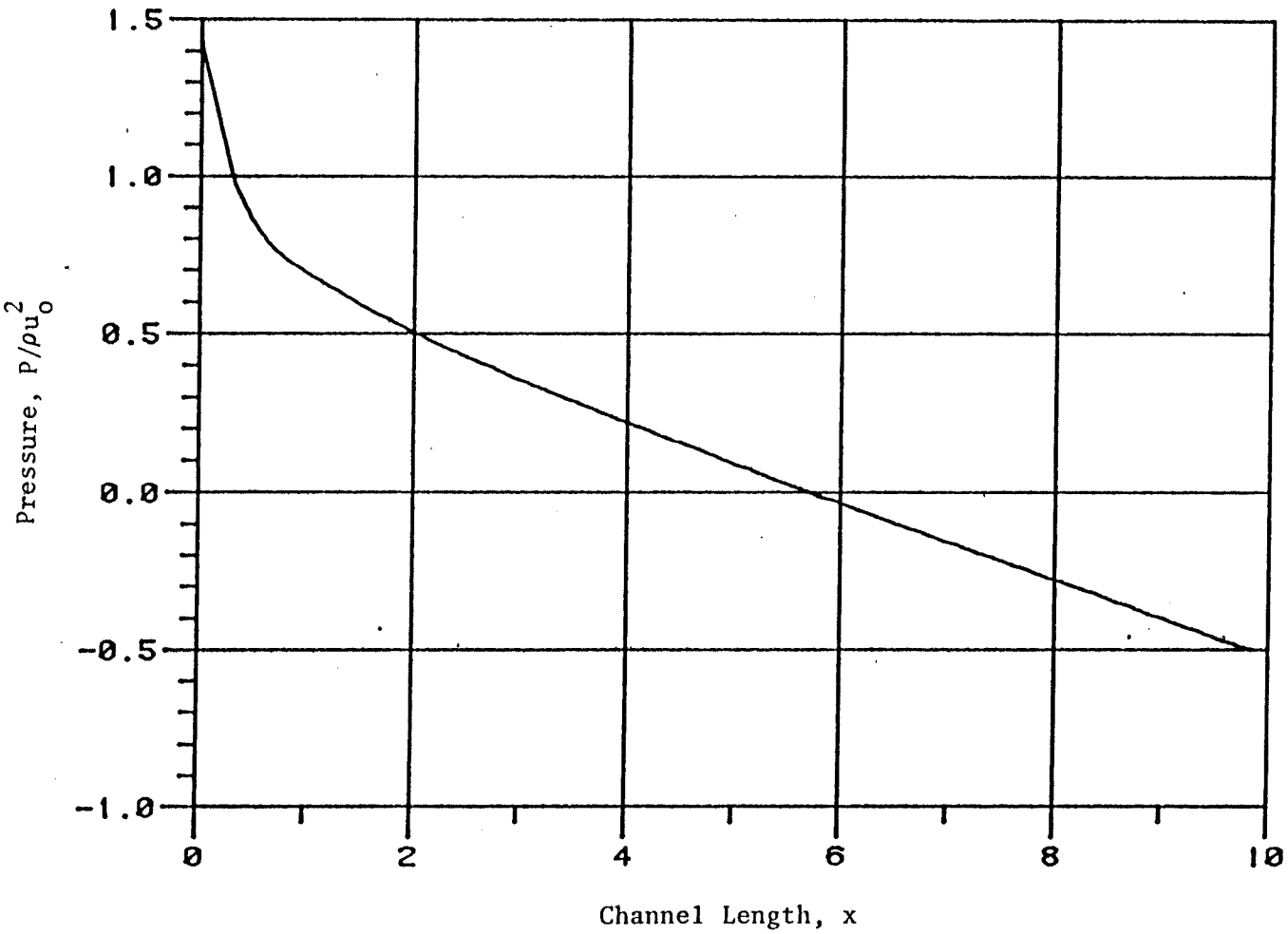

Fig. 2b Wall pressure on a straigth channel for Re=100

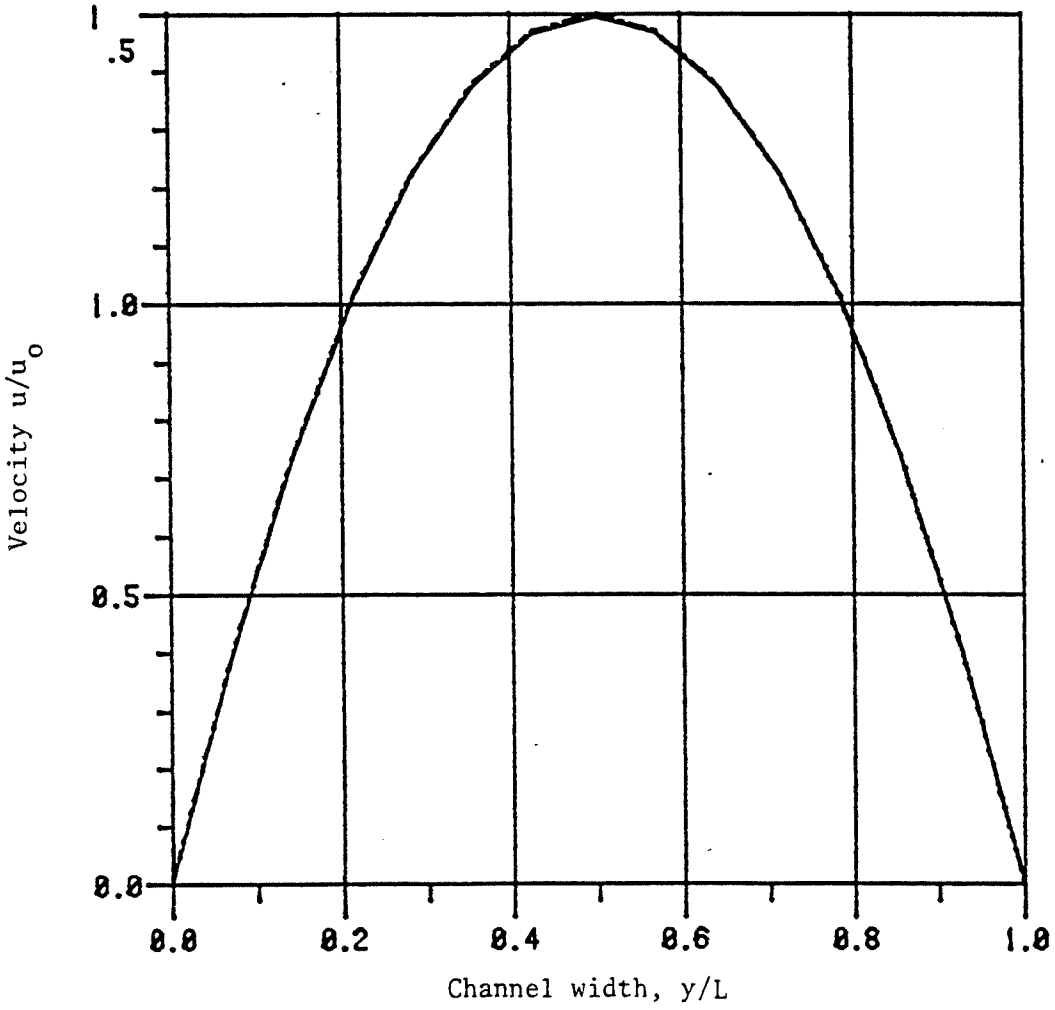

Fig. 2c Comparison of numerical and analytical velocity profiles.

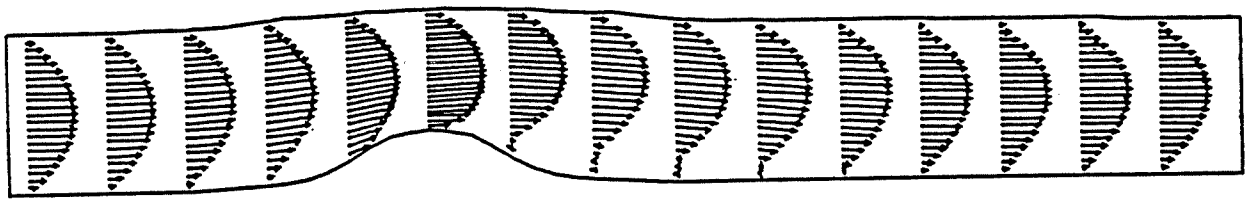

a)

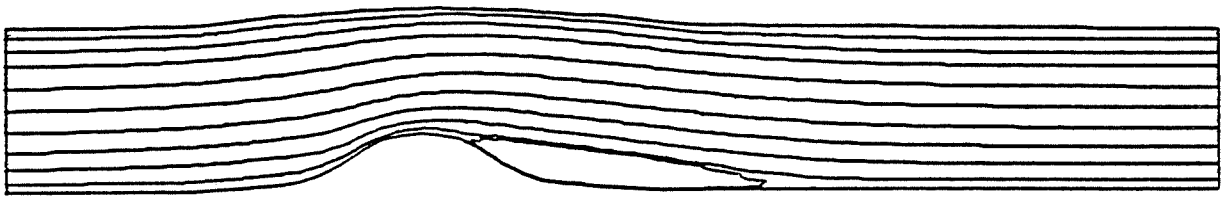

b)

Fig. 3a,3b Velocity field and stream-function contours for the geometry of Ref [12]. Re=1000

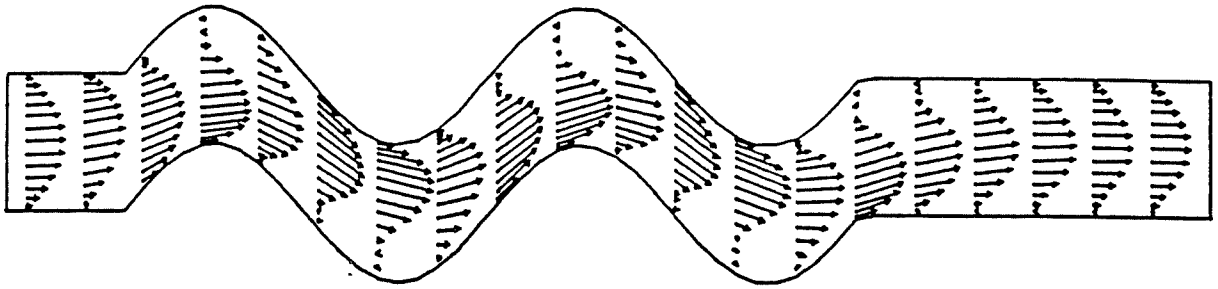

a)

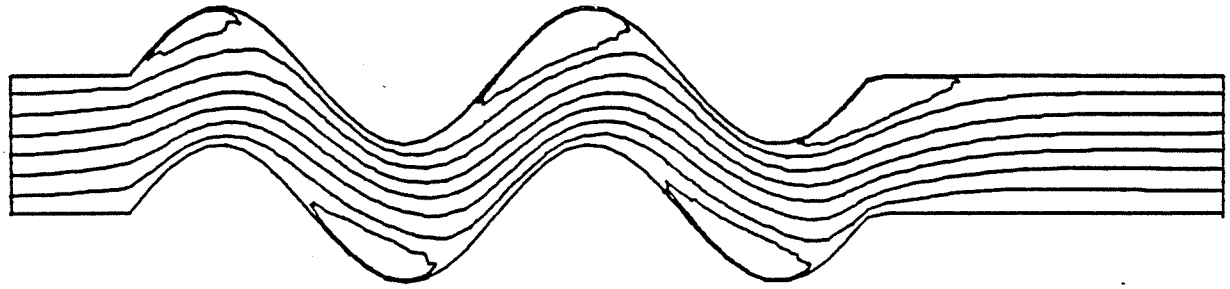

b)

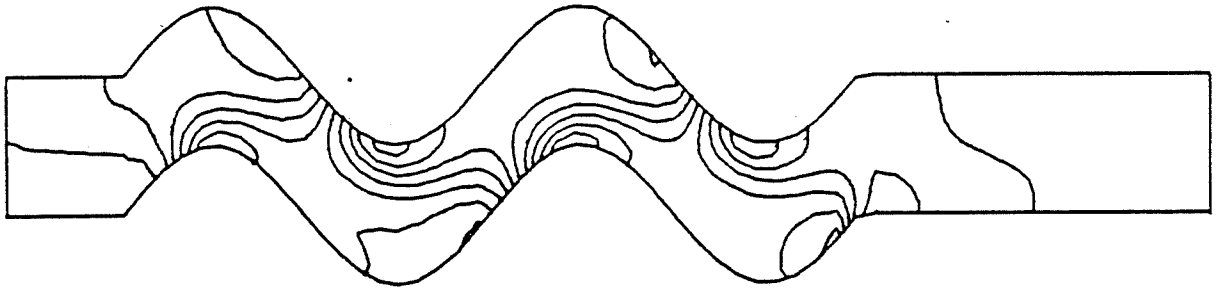

c)

Fig. 4a,4b,4c Velocity field, stream-function and isobars contours in double-sinusoidal channel. Re=100

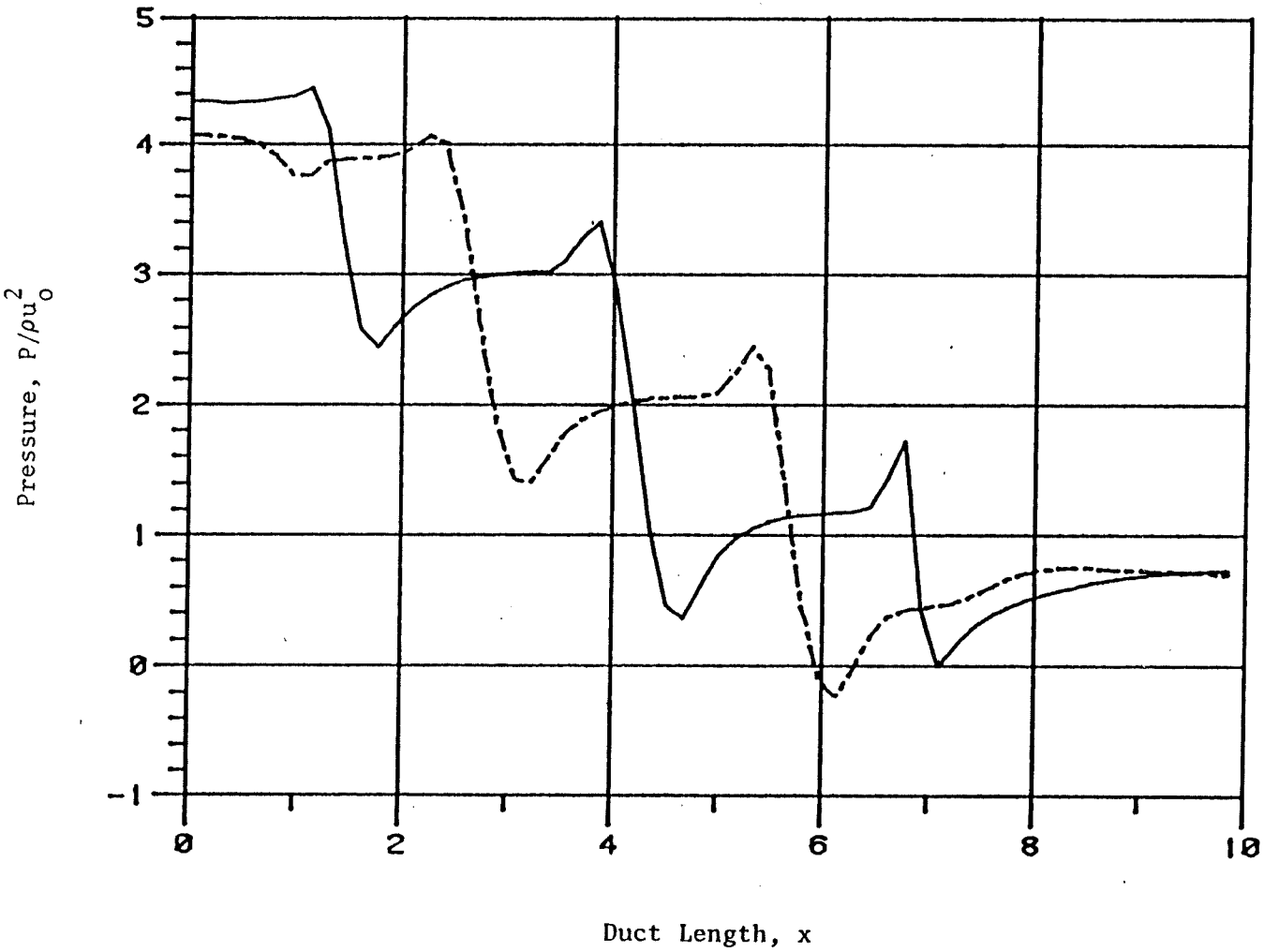

Fig. 4d Upper and lower wall pressure in a double-sinusoidal passage

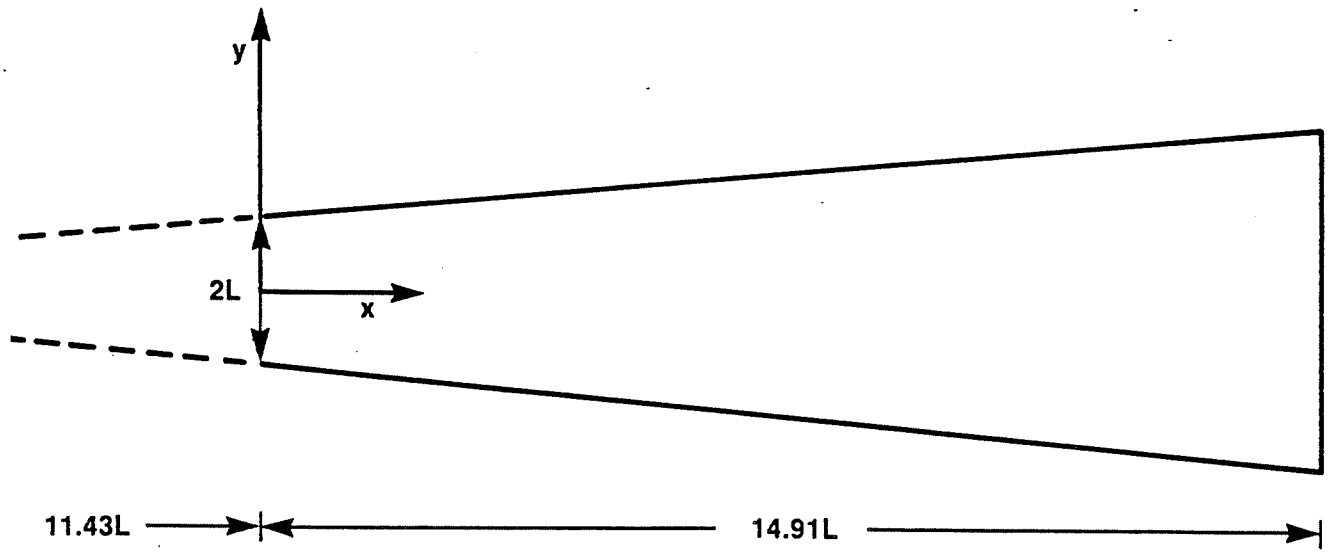

Fig. 5a Geometric characteristics of the divergent duct

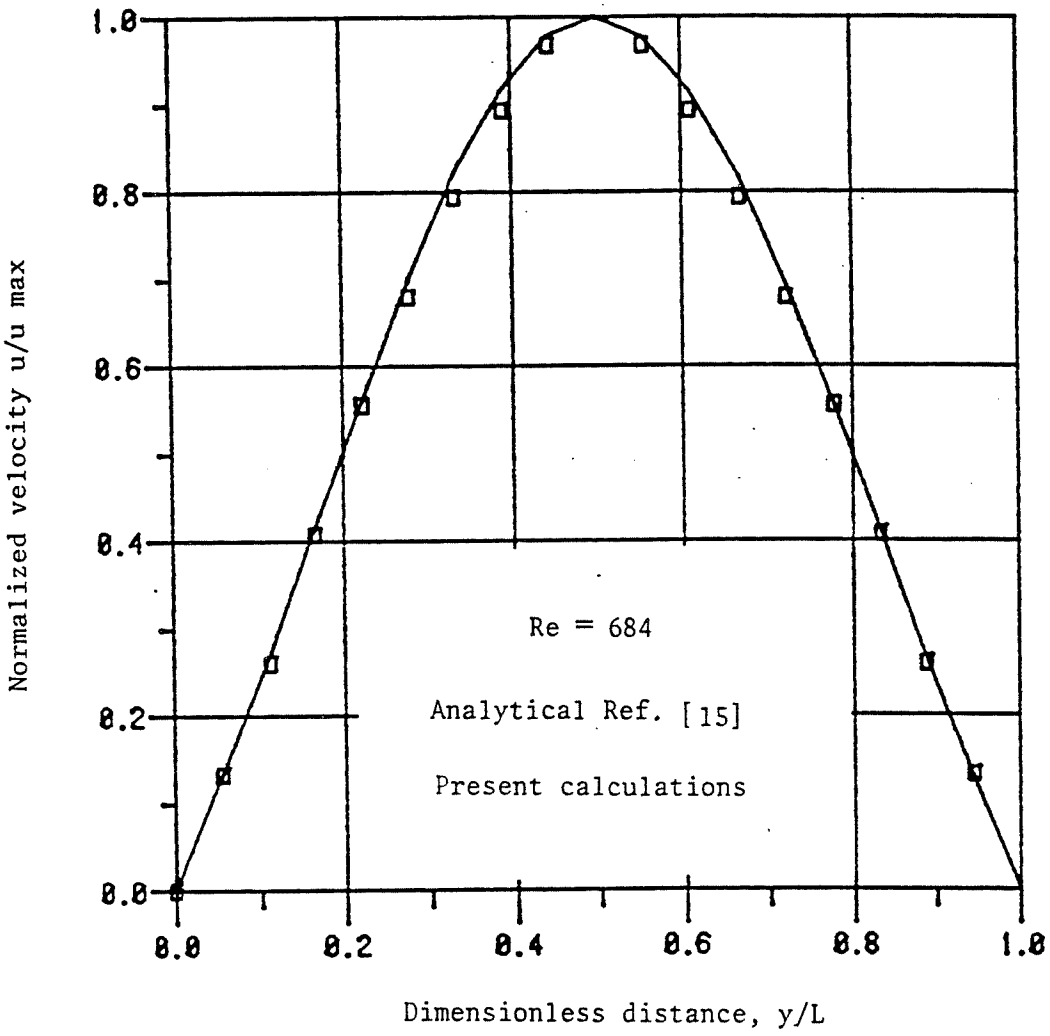

Fig. 5b Numerical and analytical solution of the Jeffery-Hamel flow. Rë=684

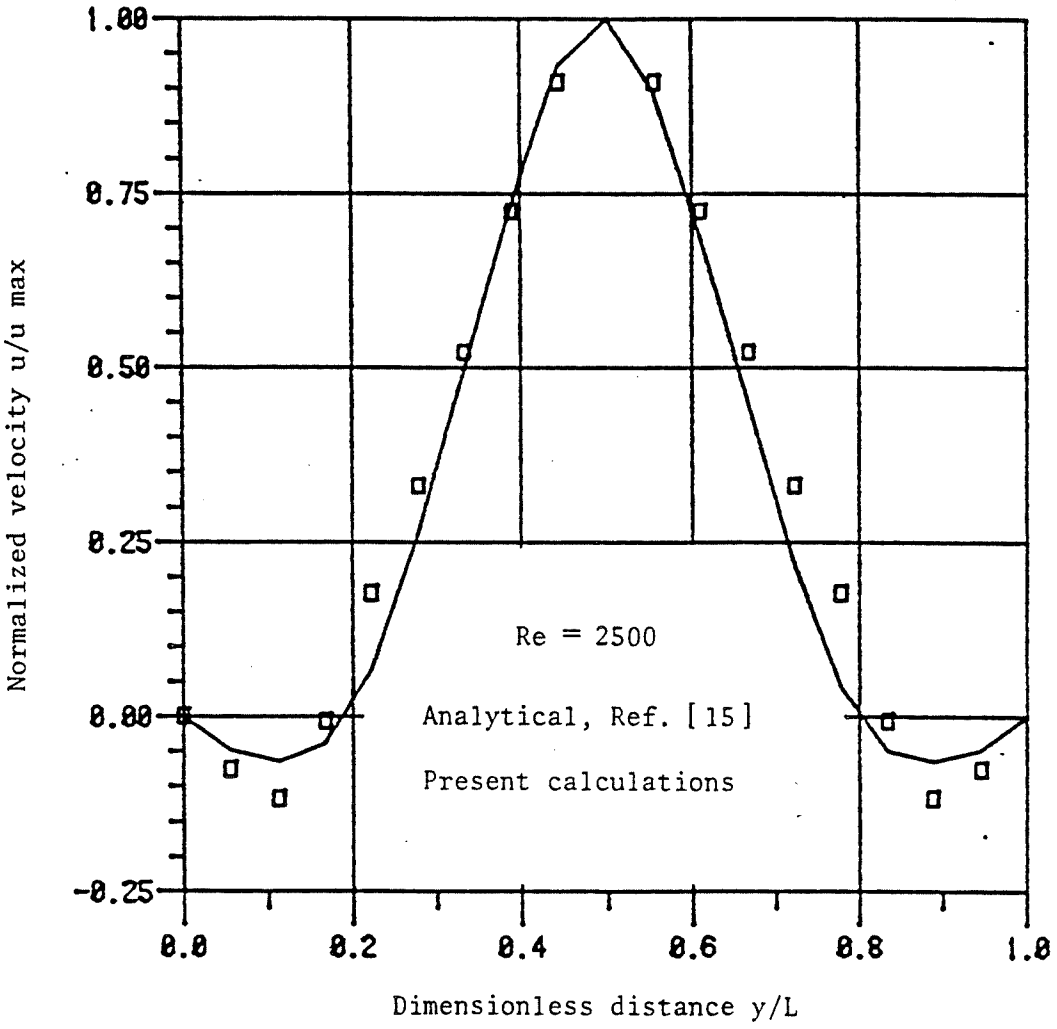

Fig. 5c Numerical and analytical solution of the Jeffery-Hamel flow. Re=2500